

Kinematic interpolation of movement data

Jed A. Long^{1*}

¹Department of Geography & Sustainable Development
School of Geography and Geosciences
University of St Andrews

*Corresponding author email: jed.long@st-andrews.ac.uk

Pre-print of published version.

Reference:

Long, JA. 2015. Kinematic interpolation of movement data. International Journal of Geographical Information Science.

DOI:

<http://dx.doi.org/10.1080/13658816.2015.1081909>

Disclaimer:

The PDF document is a copy of the final version of this manuscript that was subsequently accepted by the journal for publication. The paper has been through peer review, but it has not been subject to any additional copy-editing or journal specific formatting (so will look different from the final version of record, which may be accessed following the DOI above depending on your access situation).

1 **Abstract**

2 Mobile tracking technologies are facilitating the collection of increasingly large and de-
3 tailed datasets on object movement. Movement data are collected by recording an object's
4 location at discrete time intervals. Often, of interest is to estimate the unknown position
5 of the object at unrecorded time points to increase the temporal resolution of the data,
6 to correct erroneous or missing data points, or to match the recorded times between
7 multiple datasets. Estimating an objects unknown location between known locations is
8 termed path interpolation. This paper introduces a new method for path interpolation
9 termed kinematic interpolation. Kinematic interpolation incorporates object kinematics
10 (i.e., velocity and acceleration) into the interpolation process. Six empirical datasets (two
11 types of correlated random walks, caribou, cyclist, hurricane, and athlete tracking data)
12 are used to compare kinematic interpolation to other interpolation algorithms. Results
13 showed kinematic interpolation to be a suitable interpolation method with fast moving
14 objects (e.g., the cyclist, hurricane, and athlete tracking data), while other algorithms
15 performed best with the correlated random walk and caribou data. Several issues associ-
16 ated with path interpolation tasks are discussed along with potential applications where
17 kinematic interpolation can be useful. Finally, code for performing path interpolation is
18 provided (for each method compared within) using the statistical software R.

19 1. Introduction

20 New devices are providing scientists with unprecedented data on the movements of many
21 different types of objects (e.g., humans, vehicles, and wildlife). Movement data are typi-
22 cally collected by recording an objects location at discrete time intervals, typically rep-
23 resented by the triple $\{x, y, t\}$, where x and y are spatial coordinates, and t is the
24 time when the coordinates were recorded (Hornsby and Egenhofer 2002). Modern de-
25 vices record movement data at increasingly detailed spatial and temporal resolutions,
26 moving towards a continuous representation of the movement trajectory (Laube *et al.*
27 2007). With the rapid growth in availability of movement data, the field of GIScience
28 has made significant contributions to methods for storing, indexing, visualizing, and
29 analysing movement data, but yet there remain many areas for improving movement
30 related research (Long and Nelson 2013a, Purves *et al.* 2014).

31 Movement analysis must consider that movement data are represented discretely, and
32 thus the data represent only a sample of the object's true trajectory. When analysing
33 movement data, problems can arise where data are missing, erroneous, or sampled with
34 an irregular frequency (Laube and Purves 2011). In these cases, there is often a desire
35 to estimate an objects unknown location using known data. The process of estimating
36 unknown locations of a moving object along its trajectory is termed *path interpolation*.
37 Methods for path interpolation have many practical applications in the analysis of moving
38 objects. For example, researchers are commonly wishing to increase the temporal resolu-
39 tion of moving-object databases (Güting and Schneider 2005), often termed up-sampling
40 (Turchin 1998). Up-sampling (and down-sampling) is useful, for example, when exam-
41 ining scale-dependencies in movement pattern indices (Laube and Purves 2011). Many
42 methods for analysing joint movement patterns (e.g., Laube *et al.* 2005, Shirabe 2006,

43 Benkert *et al.* 2008, Long and Nelson 2013b) require that the temporal sampling of mul-
44 tiple datasets match-up. In cases where multiple movement datasets do not perfectly
45 match, path interpolation methods are useful for aligning the sampling resolutions of
46 two or more movement datasets. Finally, path interpolation is used widely to deal with
47 missing or erroneous data, which are commonly encountered in practice (Tremblay *et al.*
48 2006, Lonergan *et al.* 2009).

49 To date several methods have been proposed for path interpolation. The most com-
50 monly applied interpolation method is linear interpolation, which assumes that movement
51 follows the straight-line path (bee-line) between two known points. Linear interpolation
52 is advantageous because it can be straightforwardly implemented. The straight-line path
53 between two points also represents the most-likely path of movement derived from ran-
54 dom walk models (Winter and Yin 2010), making a strong theoretical argument for linear
55 interpolation as well. Random-walk models have also been used to interpolate the move-
56 ments of some animals, which are known to exhibit more random movement patterns
57 (Wentz *et al.* 2003, Technitis *et al.* 2015). However, with many types of objects linear and
58 random-walk models are inappropriate. For example, curvi-linear shapes (i.e., modelled
59 using cubic-splines or Bézier curves) have been shown to be better at interpolating the
60 movement trajectories of marine mammals (Tremblay *et al.* 2006). Similarly, Yu and Kim
61 (2004, 2006) showed that polynomial curves improved interpolation of vehicle trajectories
62 in comparison with linear interpolation methods.

63 The study of motion is commonly termed *kinematics* – which involves the use of a
64 set of kinematic equations to describe the motion properties of an object (i.e., position,
65 velocity, and acceleration) without considering the forces behind the motion. To date,
66 the most significant advances in studying kinematic properties of moving-objects within
67 GIScience have been extensions to Hägerstrand’s (1970) classic time geographic model.

68 Kuijpers *et al.* (2011) provided the mathematical framework for altering the boundaries
69 of the space–time cone and space–time prism to account for kinematic effects. Long *et al.*
70 (2014a) extended the work of Winter and Yin (2010, 2011) to construct a probabilistic
71 time–geographic model for calculating internal kinematic movement probabilities for the
72 kinematic space–time cone. The approaches developed by both Kuijpers *et al.* (2011) and
73 Long *et al.* (2014a) both fail to demonstrate how to delineate a kinematic path within a
74 kinematic space–time prism. Current approaches to path interpolation fail to adequately
75 consider the kinematic properties of the object, despite the fact that in many cases the
76 kinematic characteristics of an object will influence the movement trajectory.

77 In this paper a new method is proposed for kinematic path interpolation that can be
78 used to estimate the kinematic trajectory of an object from movement data. Here, it is hy-
79 pothesized that kinematic path interpolation will be useful with datasets representing the
80 movement of fast–moving objects, where data are collected with relatively fine sampling
81 resolutions, for example with vehicles, cyclists, or athletes. The algorithm for perform-
82 ing kinematic path interpolation is derived and six empirical datasets are demonstrated
83 to compare kinematic path interpolation with common existing approaches. Finally, a
84 discussion of the results and general points for utilizing kinematic interpolation in other
85 applications is provided.

86 2. Methods

87 The methods section begins with the development of the proposed kinematic interpola-
88 tion method. Next, descriptions of four other commonly employed interpolation methods
89 (Table 1) are provided for comparison: linear interpolation, constrained random walk,
90 Bézier curves, and Catmull-Rom curves. These methods were chosen as they reflect the

91 diversity of currently available methods for path interpolation, and are employed in a
 92 variety of situations. A contrived example is used to demonstrate each approach. Then,
 93 six empirical datasets are described which are used in order to evaluate the effectiveness
 94 of each interpolation method. The methods for evaluating each interpolation method are
 95 introduced, followed by a discussion of the computational efficiency of each method.

96 [Table 1 here]

97 **2.1. Kinematic Path Interpolation**

98 Consider the well documented situation where a moving object's position is recorded at
 99 discrete time intervals denoted $\mathbf{z}(t)$. The goal of path interpolation is to estimate the ob-
 100 ject's unknown location at some time t_u between known locations $\mathbf{z}(t_i)$ and $\mathbf{z}(t_j)$ where
 101 $t_i < t_u < t_j$. In order to perform kinematic interpolation we assume that the object
 102 has a known (or estimated) instantaneous velocity at time t_i (resp. t_j), denoted $\mathbf{v}(t_i)$
 103 (resp. $\mathbf{v}(t_j)$). Kinematic interpolation builds from the equations that define kinematic
 104 motion in one dimension, that is $\mathbf{z}(t)$ and $\mathbf{v}(t)$ are segmented into 2 (or 3) independent
 105 dimensions (i.e., $\mathbf{z}(t) = (z_x(t), z_y(t))$ and $\mathbf{v}(t) = (v_x(t), v_y(t))$). Kinematic motion equa-
 106 tions are straightforwardly extended to the 2-dimensional case by solving the system
 107 independently for each of the x and y components. The following kinematic equations
 108 can be used to describe kinematic motion in one dimension:

$$\text{position: } z(t_u) = z(t_i) + \int_{t_i}^{t_u} v(t) dt \quad (1)$$

109

$$\text{velocity: } v(t_u) = v(t_i) + \int_{t_i}^{t_u} a(t) dt \quad (2)$$

110

$$\text{acceleration: } a(t_u) = f(t_u) \quad (3)$$

111 where $f(t_u)$ is a function that describes the object's acceleration between t_i and t_j .
 112 Acceleration can change instantaneously, thus there are infinitely many ways in which
 113 we could describe an object's acceleration (and subsequently motion) via $f(t_u)$. Here
 114 it is proposed that $f(t_u)$ be modelled as a linear function of time in order to describe
 115 object acceleration as a smooth motion (i.e., no abrupt changes in speed or direction).
 116 This means that $f(t_u)$ describes the change in velocity between the two known locations
 117 as a monotonously increasing or decreasing linear function depending on $v(t_i)$ and $v(t_j)$.
 118 Specifically, $f(t_u)$ takes the form:

$$f(t_u) = b + m(t_u - t_i) \quad (4)$$

119 where b and m are two unknown parameters that represent the intercept and slope of
 120 the acceleration function. Back substitution of (4) into (1), (2), and (3) results in the
 121 equations:

$$z(t_u) = z(t_i) + v(t_i)(t_u - t_i) + \frac{b}{2}(t_u - t_i)^2 + \frac{m}{6}(t_u - t_i)^3 \quad (5)$$

122

$$v(t_u) = v(t_i) + b(t_u - t_i) + \frac{m}{2}(t_u - t_i)^2 \quad (6)$$

123

$$a(t_u) = b + m(t_u - t_i) \quad (7)$$

124 Given known values for $z(t_i)$, $z(t_j)$, $v(t_i)$, and $v(t_j)$ equations (5–7) can be used to set

125 up a system of two equations in order to solve for the parameters b and m following:

$$v(t_j) - v(t_i) = b(t_j - t_i)^2 + \frac{m}{2}(t_j - t_i)^2 \quad (8)$$

126

$$z(t_j) - z(t_i) - v(t_i)(t_j - t_i) = \frac{b}{2}(t_j - t_i)^2 + \frac{m}{6}(t_j - t_i)^3 \quad (9)$$

127 Solving the system of equations described by equations (8) and (9) for b and m allows us
 128 to back-substitute b and m into (5) in order to interpolate the position of the object at
 129 time t_u . Once b and m are solved for, equation (5) can be applied recursively to estimate a
 130 continuous kinematic trajectory between $z(t_i)$ and $z(t_j)$. As stated previously, the process
 131 described by equations (1) to (9) is applied independently to each (spatial) dimension,
 132 and thus the parameters b and m are likely to be different across different dimensions.

133 2.2. Linear interpolation

134 Linear interpolation is conducted by estimating an object's unknown location along the
 135 straight-line path between two known locations (the bee-line). Linear interpolation has
 136 been implemented in numerous studies (e.g., Wentz *et al.* 2003, Delgado *et al.* 2014,
 137 Nelson *et al.* 2015), due to its straightforward calculation and interpretation. An unknown
 138 location at a specified time $z(t_u)$ is calculated following:

$$\mathbf{z}(t_u) = \mathbf{z}(t_i) + \frac{t_u - t_i}{t_j - t_i} (\mathbf{z}(t_j) - \mathbf{z}(t_i)) \quad (10)$$

139 Linear interpolation is a special case of kinematic interpolation where it is assumed that
 140 $\mathbf{v}(t_i) = \mathbf{v}(t_j) = \frac{\mathbf{z}(t_j) - \mathbf{z}(t_i)}{t_j - t_i}$ (i.e., constant motion) such that the parameters $b = m = 0$.

141 **2.3. Constrained Random Walk**

142 Random walks can be used to interpolate a moving object, whereby an interpolated
143 position is dependent on the previous position. Random walks are generated by taking
144 random samples from two distributions: a step-length distribution (l) and a turning
145 angle distribution (θ) (Turchin 1998). The coordinates for a random walk position can
146 be calculated simply as $z_x(t_u) = z_x(t_i) + l \cos(\theta)$ and $z_y(t_u) = z_y(t_i) + l \sin(\theta)$ (Turchin
147 1998). Such a random walk approach fails to consider the sequential nature of movement
148 data, that is, that the object travels between two consecutive known locations $\mathbf{z}(t_i)$
149 and $\mathbf{z}(t_j)$. Thus, here a specific type of random walk is chosen, where the interpolation
150 is constrained to the time geographic space-time prism (Hägerstrand 1970). Using the
151 space-time prism to constrain random walks was first employed by Wentz *et al.* (2003),
152 and further developed by Technitis *et al.* (2015), both in the context of interpolating
153 paths from wildlife tracking data. As the object must move from location $\mathbf{z}(t_i)$ to $\mathbf{z}(t_j)$
154 the space-time prism is used to constrain the potential points included in the random
155 walk (i.e., it is not completely random). To calculate such a constrained random walk,
156 the potential point area for t_u is computed by intersecting the forward and past space-
157 time cones from t_i to t_u and t_j to t_u respectively (Technitis *et al.* 2015). The constrained
158 random walk algorithm is implemented by randomly selecting a location within the
159 potential point area for t_u . When more than one point is to be interpolated, the time
160 geographic constrained random walk algorithm accounts for the tendency of a random
161 walk to wander around the first point and then make a bee-line to the second point
162 (Wentz *et al.* 2003, Technitis *et al.* 2015) by randomly ordering the t_u 's to be interpolated.
163 The algorithm requires a parameter (v_{max}) representing the upper bound on mobility
164 (i.e., velocity) which here was estimated as the maximum of either the 25th percentile
165 of all segment velocities or $1.25 \times$ the observed segment velocity between t_i and t_j to

166 account for differences between faster and slower movement periods. For more details on
 167 the time geographic constrained random walk see Technitis *et al.* (2015).

168 **2.4. Bézier Curve**

169 A cubic Bézier curve algorithm has been shown to be an effective interpolation method
 170 for some types of moving objects (Tremblay *et al.* 2006). Calculating the cubic Bézier
 171 curve requires definition of four anchor points, two of which are the origin $P_1 = \mathbf{z}(t_i)$
 172 and destination point locations $P_4 = \mathbf{z}(t_j)$, and the other two (P_2, P_3) control the shape
 173 of the curve. Here, the approach taken for computing the Bézier control points (P_2, P_3)
 174 is based on the initial and exit velocities (see below). Such an approach makes the Bézier
 175 curve (as implemented here) comparable with kinematic interpolation, in that they use
 176 the same information.

$$P_2 = \mathbf{z}(t_i) + \mathbf{v}(t_i) \frac{1}{2}(t_j - t_i) \quad (11)$$

$$P_3 = \mathbf{z}(t_j) - \mathbf{v}(t_j) \frac{1}{2}(t_j - t_i) \quad (12)$$

$$\mathbf{z}(t_u) = (1 - \delta)^3 P_1 + 3(1 - \delta)^2 \delta P_2 + 3(1 - \delta) \delta^2 P_3 + \delta^3 P_4 \quad (13)$$

177 where $\delta = \frac{t_u - t_i}{t_j - t_i}$, δ being simply the time we wish to interpolate scaled to unity.

178 2.5. *Catmull-Rom Curve*

179 Another curve-based option is the Catmull-Rom curve (Barry and Goldman 1988, Yuksel
 180 *et al.* 2011) which is a special type of cubic-spline that can be used to straightforwardly
 181 interpolate between known data points. The principal advantage of the Catmull-Rom
 182 curve approach in the context of path interpolation is that the observed movement loca-
 183 tions are used directly as control points for the interpolated curve. Catmull-Rom curves
 184 can be used to estimate the location of an object at t_u based on four control points
 185 defined by $\mathbf{z}(t_{i-1}), \mathbf{z}(t_i), \mathbf{z}(t_j), \mathbf{z}(t_{j+1})$ (see Supplementary Material A for derivation).

186 2.6. *Example*

187 To demonstrate kinematic interpolation, a contrived example is used to compare the
 188 interpolated locations from the kinematic algorithm to the other methods. In this con-
 189 trived scenario, consider a sequence of four points, where an object begins at the point
 190 $\mathbf{z}(0) = (0, -3)$ with a velocity of 0 m/s and then moves to the origin $\mathbf{z}(1) = (0, 0)$ with a
 191 velocity of 3 m/s to the North $\mathbf{v}(1) = (0, 3)$. The object reaches position $\mathbf{z}(6) = (10, 10)$
 192 after 5 s , it now has a velocity of 3 m/s to the East $\mathbf{v}(6) = (3, 0)$ and it continues on
 193 to location $\mathbf{z}(7) = (13, 10)$. Using each interpolation method the location of the object
 194 is estimated at $1/2 \text{ s}$ intervals from $t_u = 1$ to 6 s in order to show the shape of the
 195 interpolated trajectory resulting from each method (Figure 1).

196 [Figure 1 here]

197 The differences between each interpolation method and the kinematic interpolation
 198 method proposed are readily observed from this contrived example. The linear interpo-
 199 lation algorithm follows the ‘bee-line’ path between the two known points (Figure 1a).
 200 The constrained random walk wanders within the space in between the known points

201 as defined by the space-time prism (Figure 1b). The Bézier method results in a curved
202 trajectory that is more exaggerated than the kinematic path, but one that seems to
203 incorporate the initial and final velocities (Figure 1c). The Catmull-Rom curve is the
204 closest to the kinematic curve, in this case, with only small differences observed (Figure
205 1d).

206 **2.7. Data**

207 Six empirical datasets are used to compare and contrast the new kinematic path interpo-
208 lation algorithm with the other methods (Figure 2). The first two datasets are generated
209 via simulations using correlated random walks that exhibit a low ($r = 0.2$) or high
210 ($r = 0.9$) level of correlation in movement. Correlated random walks are commonly used
211 to model animal movement, and have been used in many studies (e.g., Fauchald and
212 Tveraa 2003, Rowcliffe *et al.* 2012, Long *et al.* 2014b) to compare different methods for
213 analysing movement data. The third dataset tracks the movement of a caribou in north-
214 ern British Columbia, Canada over a one year period. Caribou locations were recorded
215 every 4 *h* using satellite telemetry. The fourth dataset represents the movement of a
216 cyclist within an urban environment. Cyclist locations were recorded using a GPS with
217 a 1/5 *Hz* sampling rate. The fifth dataset shows the movement of hurricane Katrina at
218 3 *h* intervals between 21:00 on 26-Aug-2005 and 21:00 29-Aug-2005. The point location
219 of the hurricane was calculated as the centroid of the eye of the hurricane, obtained from
220 the NOAA H*WIND data product (Powell *et al.* 1998, 2010). The final dataset shows
221 the movement of an athlete playing Ultimate Frisbee. The athlete tracking data were
222 recorded using a sport-specific GPS device (GPSports, Fyshwick, Australia) with a 5
223 *Hz* sampling rate.

224 [Figure 2 here]

225 2.8. Interpolation Testing

226 In order to test the effectiveness of each path interpolation algorithm an approach similar
227 to previous interpolation studies (e.g., Wentz *et al.* 2003, Tremblay *et al.* 2006) is fol-
228 lowed. A known point $z(t_k)$ (or sequence of points, $k \in \{1, 2, 3, \dots\}$) is removed and then
229 estimated via interpolation from the surrounding points. Thus, the procedure utilizes a
230 sequential moving window approach to removing k known points and subsequently re-
231 estimating them by each of the five interpolation methods (a similar approach to Long
232 *et al.* 2014a). As the number of consecutive fixes to be estimated (k) is increased the
233 interpolation task becomes more difficult.

234 With some tracking devices instantaneous velocities may be recorded alongside the
235 location points, but typically this is not the case. In cases where instantaneous velocities
236 are unknown, the initial velocity $\mathbf{v}(t_i)$ and final velocity $\mathbf{v}(t_j)$ can be estimated using the
237 distance between two consecutive fixes and dividing it by the time difference. Specifically
238 here instantaneous velocities are estimated for $\mathbf{v}(t_i)$ and $\mathbf{v}(t_j)$ using the observed tracking
239 data. That is, $\mathbf{v}(t_i) = \frac{\mathbf{z}(t_i) - \mathbf{z}(t_{i-1})}{t_i - t_{i-1}}$ and $\mathbf{v}(t_j) = \frac{\mathbf{z}(t_{j+1}) - \mathbf{z}(t_j)}{t_{j+1} - t_j}$.

240 To evaluate interpolation performance two measures of overall assessment are used.
241 The first measure is the root mean squared error (rmse) of the error between the in-
242 terpolated locations and the known points, where error is defined simply as the spatial
243 euclidean distance between an interpolated point estimate and the known location. The
244 second measure is the proportion of the points in the interpolation where a given method
245 performed best (P_{best}). The P_{best} measure is comparative, allowing direct comparison be-
246 tween the five methods for each interpolated location. To test across a range of interpo-
247 lation difficulties, the interpolation testing procedure described above was implemented
248 on each of the six datasets using values of k ranging from $k = 1, \dots, 10$, representing
249 increasing interpolation difficulty.

250 **2.9. Examination of Computational Efficiency**

251 The complexity of each method was investigated, along with a time-trial, to examine the
252 computational efficiency of each method. All analysis was conducted using the statistical
253 computing software R (R Development Core Team 2015), and the code for each algorithm
254 is available in the Supplementary Material. To test the computational efficiency of each
255 algorithm a scenario was derived (similar to that in the contrived example) where the
256 number of points to be interpolated was set to $k = 1 \times 10^6, 1 \times 10^7, 1 \times 10^8$, and 2×10^8 . Each
257 scenario was run 100 times, and the average of these runs is reported in Supplementary
258 Material B. In the case of the constrained random walk, the algorithm is much slower,
259 and for comparison $k = 1 \times 10^1, 1 \times 10^2, 1 \times 10^3$, and 2×10^3 was used. The results were
260 realised on a standard desktop PC (Intel QuadCore i7 3770 CPU @ 3.40 GHz, with 16
261 Gb of RAM, on Windows 7) running R version 3.1.2.

262 **3. Results**

263 **3.1. Interpolation Testing**

264 For the first correlated random walk (CRW1) the linear method had the lowest rmse,
265 while the time geographic constrained random walk had the highest rmse, for all values of k
266 (Figure 3a). As would be expected, the level of rmse increased with k for all methods, and
267 this was consistent across the different datasets. With the more correlated (i.e., smoother)
268 random walk (CRW2) the linear, kinematic, and Catmull-Rom curve methods provided
269 nearly identical results, and the kinematic and Catmull-Rom curve methods resulted in
270 lower rmse at higher values of k (Figure 3b). With the caribou data, the linear method
271 resulted in the lowest rmse, followed by the Catmull-Rom method. With the caribou
272 data, the Bézier curve method (Figure 3c) showed the highest rmse. With the cyclist

273 data the kinematic and Catmull-Rom methods performed nearly identically, with the
274 lowest rmse, followed by the Bézier, linear, and constrained random walk (Figure 3d). In
275 the hurricane Katrina dataset, again the Catmull-Rom and kinematic methods performed
276 similarly, but for larger k these two methods resulted in much lower rmse than the other
277 three methods (Figure 3e). Finally for the athlete dataset at low k values the linear,
278 Catmull-Rom, and kinematic methods perform nearly identical, but as k increases, the
279 kinematic and the Catmull-Rom methods have lower rmse than the linear, and other
280 methods (Figure 3f).

281 [Figure 3 here]

282 Looking at the P_{best} measure of fit, in CRW1 linear had the best fit for about 40% of the
283 interpolation points, while constrained random walk was best in about 30% of the points
284 (Figure 4a). With CRW2 linear had the best fit about 30–40% of the points, while Bézier
285 was best at higher values of k (Figure 4b). The linear method performed even better with
286 the caribou data, having the P_{best} estimate upwards of 40% of the interpolations, while
287 the constrained random walk had 30% and the other methods around 10% each (Figure
288 4c). In the cyclist data, the linear and Catmull-Rom were very close for $k = 1$ with P_{best}
289 about 30% each, however as k increases the kinematic method produced similarly good
290 results (Figure 4d). With the hurricane Katrina dataset a more unpredictable pattern
291 emerges; at low values for k the linear method had the highest P_{best} values, while for
292 higher k the Catmull-Rom, and kinematic method performed better (Figure 4e). In the
293 athlete data, the linear method performed best with $P_{best} \simeq 40\%$ with $k = 1$, but at higher
294 k the Catmull-Rom and kinematic methods again were best performing approximately
295 equally well (Figure 4f).

296 [Figure 4 here]

297 **3.2. Computational Efficiency**

298 Each of the five methods employed here are $O(n)$ complex. The linear, Bézier curve,
299 Catmull-Rom curve, and kinematic methods are all relatively fast and easy to com-
300 pute (see Supplementary Material B). The linear method is the fastest, followed by the
301 Catmull-Rom curve, then kinematic, and finally the Bézier curve, but the differences
302 between these four are negligible in practical scenarios (e.g., 1×10^6 interpolations in
303 < 1 second). The constrained random walk method, however, takes much longer (e.g.,
304 the time taken for interpolating 10 points using the constrained random walk method
305 was comparable to interpolating 1×10^6 points using the other methods). This difference
306 is likely due to the additional requirement of intersecting the forward and past space-
307 time cones for each interpolation which is a computationally expensive operation (more
308 information on the performance of constrained random walk algorithm can be found
309 in Technitis *et al.* 2015). Thus, kinematic interpolation is a fast and computationally
310 efficient interpolation method, in-line with, or better than, existing approaches.

311 **4. Discussion**

312 With different types of movement processes different models are expected to be more ap-
313 propriate. As hypothesized, the kinematic interpolation method performed best with fast
314 moving objects where kinematic properties are known to influence movement (e.g., cy-
315 clists and athletes). With cyclists it is somewhat surprising that kinematic outperformed
316 linear interpolation given the linear shape of cyclist movement along road networks.
317 This result is owed to the effect of changes in speed (e.g., slowing down or speeding up),
318 which are appropriately modelled via kinematic interpolation and are ignored in the lin-
319 ear method. It was also found that kinematic interpolation may be useful for other types

320 of objects, for example hurricane movements as shown here. Recent studies have focused
321 on analysing spatial-temporal patterns in large collections of hurricane tracks (Dodge
322 *et al.* 2012, Buchin *et al.* 2012). Here kinematic interpolation may provide a useful tool
323 for up-sampling such analysis or comparing data with differing temporal resolutions.
324 Here, the similar, but different outcomes of three curve-based interpolation algorithms:
325 Bézier curves, Catmull-Rom curves, kinematic interpolation, are clearly demonstrated.
326 Our results suggest that Catmull-Rom and kinematic curves are nearly equivalent, and
327 most appropriate with fast-moving objects, producing very similar rmse values in the
328 empirical examples shown. Bézier curves are likely more useful only in specific scenarios,
329 which is surprising given that they performed well in the study by Tremblay *et al.* (2006).

330 It may be unsurprising that the curve-based methods (i.e., Bézier and Catmull-Rom)
331 and kinematic method out-performed linear interpolation. One reason for this is that the
332 Bézier, Catmull-Rom, and kinematic methods all take into consideration the surrounding
333 points in some way. Here, the surrounding points (i.e., $\mathbf{z}(t_{i-1})$ and $\mathbf{z}(t_{j+1})$) were used
334 to estimate the initial velocities used in both the Bézier and kinematic methods. In the
335 Catmull-Rom algorithm, the points $\mathbf{z}(t_{i-1})$ and $\mathbf{z}(t_{j+1})$ are used directly in the calcula-
336 tion. The constrained random walk, also uses ancillary information in the form of the
337 v_{max} parameter. In this sense the comparisons made here are somewhat unfair to the
338 linear method, as it uses the least amount of information in its calculation.

339 Movement data are typically recorded as discrete (i.e., x, y, t) points and analysis meth-
340 ods are then influenced by the granularity (i.e., temporal resolution) at which data are
341 collected. The equations for kinematic motion, as implemented here, assume accelera-
342 tion to be a linear function of time. This assumption is reasonable when movement data
343 are recorded at relatively high sampling resolutions (i.e., the cyclist data and athlete
344 data here). The idea that two consecutive points in a movement dataset can be related

345 to each other through kinematic equations can be thought of as *kinematic dependence*.
346 With many movement data examples, the assumption of kinematic dependence is unre-
347 alistic, for example here with caribou data collected at temporal resolution of 4 h. With
348 data where kinematic dependence is not present, it is unlikely that kinematic interpola-
349 tion will be useful. However, note that kinematic dependence is not entirely dependent on
350 the tracking interval. With some objects with coarse tracking intervals their kinematics
351 may still be relevant, for example, with hurricanes as shown by the hurricane Katrina
352 example. This is related to the joint effects of the objects velocity and size, along with
353 the acceleration and turning ability of the object. With athletes this concept is often
354 characterized using the term *agility*.

355 With the datasets employed here instantaneous velocities were not known and were es-
356 timated from the data. However, when instantaneous velocity is estimated from the data,
357 the velocity estimation is highly dependent on the temporal resolution of the movement
358 data (Laube and Purves 2011). The process of estimating instantaneous velocities likely
359 influenced the resulting interpolations; using an example where instantaneous velocities
360 were known would improve the performance of kinematic interpolation. In studying ma-
361 rine mammals it is useful to deploy a “dead reckoning” tag (which usually consists of
362 an accelerometer, a magnetometer, a time-depth recorder, and other components) along-
363 side GPS devices to help interpolate between fixes, as marine mammals can only be
364 tracked via GPS when they surface (Wilson *et al.* 2007, Nordstrom *et al.* 2013). Several
365 approaches have been proposed for modelling the interpolated path combining GPS and
366 accelerometer data (e.g., Wilson *et al.* 2007, Liu *et al.* 2014). Similarly, the GPS units
367 commonly used to study the movements of athletes often incorporate high frequency
368 tri-axial accelerometers into the unit (Barbero-Alvarez *et al.* 2010, Coutts and Duffield
369 2010). New approaches capable of integrating kinematic interpolation with accelerometer

370 data may provide improved estimates of fine-scale movements from tracking data where
371 both GPS and accelerometer data are recorded.

372 Perhaps the most interesting potential development from this work is the potential
373 to build upon the work of Kuijpers *et al.* (2011) and Long *et al.* (2014a) in order to
374 study kinematic probabilities within the kinematic space-time prism. Using simulated
375 kinematic trajectories, kinematic probabilities can be defined within the kinematic space-
376 time prism, where probability is defined by the amount of energy or *work* (from classical
377 mechanics, Goldstein *et al.* 2001) required to undergo a movement trajectory. Trajectories
378 requiring more *work* can be modelled as having lower movement probability in order to
379 construct a probabilistic kinematic space-time prism, similar to that proposed by Winter
380 and Yin (2010, 2011). Such developments will have the benefit of being grounded in un-
381 derlying movement theory (i.e., kinematic motion equations), and would be appropriate
382 for several types of fluid movement (e.g., athletes and hurricanes described here).

383 The results highlight the value of the traditional linear method for interpolation. Sim-
384 ply put, in many scenarios the linear method performed as well as or better than other
385 more complex methods. With animal tracking data, especially land mammals whose
386 movement are frequently modelled via random walks (Codling *et al.* 2008), the linear
387 method remains a suitable choice. Tremblay *et al.* (2006) showed that the Bézier inter-
388 polation out-performed linear interpolation with marine mammals, however, the results
389 (i.e., CRW2) suggest the kinematic or Catmull-Rom approach may be a suitable al-
390 ternative to Bézier curve methods with marine mammals and other species exhibiting
391 curvi-linear movement patterns. With moving object datasets that are both fast moving
392 and represented by data at an appropriately fine temporal resolution, kinematic inter-
393 polation is an appropriate alternative method for interpolating object locations.

394 5. Conclusion

395 This paper proposes a new method for interpolating movement data trajectories, one
396 that is based on object *kinematics*. Using several empirical datasets reflecting different
397 types of movement scenarios, this research highlights where kinematic interpolation im-
398 proves, or is comparable to, existing approaches. Further, this research demonstrates
399 situations where existing and simpler methods (i.e., linear interpolation) may be more
400 appropriate. Kinematic interpolation represents a suitable interpolation method with
401 fast moving objects, where movement data is collected at a relatively high temporal
402 resolution. Examples include cyclists, motorists, and athlete tracking data. Similarly,
403 kinematic interpolation may be useful for tracking large objects (e.g., hurricanes) that
404 display kinematic effects over broad spatial-temporal extents, or with datasets where
405 curvi-linear movement patterns are present. Finally, perhaps the biggest contribution of
406 kinematic interpolation is the opportunity for future research developing calculations for
407 kinematic movement probabilities for the space-time prism. To assist other researchers
408 wishing to perform path interpolation, code is provided (in the statistical software R)
409 for each method described herein.

410 Acknowledgements

411 References

- 412 Barbero-Alvarez, J.C., *et al.*, 2010. The validity and reliability of a global positioning
413 satellite system device to assess speed and repeated sprint ability (RSA) in athletes..
414 *Journal of science and medicine in sport / Sports Medicine Australia*, 13 (2), 232–5.
- 415 Barry, P.J. and Goldman, R.N., 1988. A recursive evaluation algorithm for a class of

- 416 Catmull-Rom splines. *ACM SIGGRAPH Computer Graphics*, 22 (4), 199–204.
- 417 Benkert, M., *et al.*, 2008. Reporting flock patterns. *Computational Geometry*, 41 (3),
418 111–125.
- 419 Buchin, M., Dodge, S., and Speckmann, B., 2012. Context-aware similarity of trajecto-
420 ries. In: N. Xiao, M.p. Kwan, M.F. Goodchild and S. Shekhar, eds. *7th International*
421 *Conference of GIScience*, 612 Columbus, OH: Springer, LNCS 7478, 43–56.
- 422 Codling, E.a., Plank, M.J., and Benhamou, S., 2008. Random walk models in biology.
423 *Journal of the Royal Society Interface*, 5 (25), 813–834.
- 424 Coutts, A.J. and Duffield, R., 2010. Validity and reliability of GPS devices for measuring
425 movement demands of team sports. *Journal of Science and Medicine in Sport*, 13,
426 133–135.
- 427 Delgado, M.D.M., *et al.*, 2014. A statistical framework for inferring the influence of
428 conspecifics on movement behaviour. *Methods in Ecology and Evolution*, 5 (2), 183–
429 189.
- 430 Dodge, S., Laube, P., and Weibel, R., 2012. Movement similarity assessment using sym-
431 bolic representation of trajectories. *International Journal of Geographical Information*
432 *Science*, 26 (1), 1563–1588.
- 433 Fauchald, P. and Tveraa, T., 2003. Using First-Passage Time in the Analysis of Area-
434 Restricted Abd Habitat Selection. *Ecology*, 84 (2), 282–288.
- 435 Goldstein, H., Poole, C., and Safko, J., 2001. *Classical Mechanics*. Third San Francisco:
436 Addison Wesley.
- 437 Güting, R.H. and Schneider, M., 2005. *Moving Objects Databases*. The Morgan Kaufmann
438 Series in Data Management Systems New York, NY: Elsevier.
- 439 Hägerstrand, T., 1970. What about people in regional science?. *Papers of the Regional*
440 *Science Association*, 24 (1), 7–21.

- 441 Hornsby, K. and Egenhofer, M.J., 2002. Modeling moving objects over multiple granu-
442 larities. *Annals of Mathematics and Artificial Intelligence*, 36 (1-2), 177–194.
- 443 Kuijpers, B., Miller, H.J., and Othman, W., 2011. Kinetic space-time prisms. *In: 19th*
444 *ACM SIGSPATIAL International Conference on Advances in Geographic Information*
445 *Systems* Nov. 1-4, Chicago, IL: Association for Computing Machinery, 162–170.
- 446 Laube, P., Imfeld, S., and Weibel, R., 2005. Discovering relative motion patterns in groups
447 of moving point objects. *International Journal of Geographical Information Science*,
448 19 (6), 639–668.
- 449 Laube, P., *et al.*, 2007. Movement beyond the snapshot Dynamic analysis of geospatial
450 lifelines. *Computers, Environment and Urban Systems*, 31 (5), 481–501.
- 451 Laube, P. and Purves, R.S., 2011. How fast is a cow? Cross-scale analysis of movement
452 data. *Transactions in GIS*, 15 (3), 401–418.
- 453 Liu, Y., *et al.*, 2014. Bayesian Melding of the Dead-Reckoned Path and GPS Measure-
454 ments for an Accurate and High-Resolution Path of Marine Mammals. 1–26.
- 455 Lonergan, M., Fedak, M., and McConnell, B., 2009. The effects of interpolation error
456 and location quality on animal track reconstruction. *Marine Mammal Science*, 25 (2),
457 275–282.
- 458 Long, J.A. and Nelson, T.A., 2013a. A review of quantitative methods for movement
459 data. *International Journal of Geographical Information Science*, 27 (2), 292–318.
- 460 Long, J.A. and Nelson, T.A., 2013b. Measuring dynamic interaction in movement data.
461 *Transactions in GIS*, 17 (1), 62–77.
- 462 Long, J.A., Nelson, T.a., and Nathoo, F.S., 2014a. Toward a kinetic-based probabilistic
463 time geography. *International Journal of Geographical Information Science*, 28 (5),
464 855–874.
- 465 Long, J.A., *et al.*, 2014b. A critical examination of indices of dynamic interaction for

- 466 wildlife telemetry studies.. *Journal of Animal Ecology*, 83 (5), 1216–1233.
- 467 Nelson, T., *et al.*, 2015. A time geographic approach for delineating areas of sustained
468 wildlife use. *Annals of GIS*, 21 (1), 81–90.
- 469 Nordstrom, C.a., *et al.*, 2013. Northern fur seals augment ship-derived ocean tempera-
470 tures with higher temporal and spatial resolution data in the eastern Bering Sea. *Deep*
471 *Sea Research Part II: Topical Studies in Oceanography*, 94, 257–273.
- 472 Powell, M.D., *et al.*, 1998. The HRD real-time hurricane wind analysis system. *Journal*
473 *of Wind Engineering and Industrial Aerodynamics*, 77-78, 53–64.
- 474 Powell, M.D., *et al.*, 2010. Reconstruction of Hurricane Katrina’s wind fields for storm
475 surge and wave hindcasting. *Ocean Engineering*, 37 (1), 26–36.
- 476 Purves, R.S., *et al.*, 2014. Moving beyond the point: An agenda for research in movement
477 analysis with real data. *Computers, Environment and Urban Systems*, 47, 1–4.
- 478 R Development Core Team, 2015. *R: A language and environment for statistical com-*
479 *puting..* Technical report, R Foundation for Statistical Computing, Vienna, Austria.
- 480 Rowcliffe, J.M., *et al.*, 2012. Bias in estimating animal travel distance: The effect of
481 sampling frequency. *Methods in Ecology and Evolution*, 3 (4), 653–662.
- 482 Shirabe, T., 2006. Correlation analysis of discrete motions. *In: M. Raubal, H.J. Miller,*
483 *A. Frank and M.F. Goodchild, eds. GIScience 2006. LNCS, vol. 4197., Vol. 4197 Berlin:*
484 *Springer-Verlag, 370–382.*
- 485 Technitis, G., *et al.*, 2015. From A to B , randomly: A point-to-point random trajectory
486 generator for animal movement. *International Journal of Geographical Information*
487 *Science.*
- 488 Tremblay, Y., *et al.*, 2006. Interpolation of animal tracking data in a fluid environment.
489 *Journal of Experimental Biology*, 209 (1), 128–140.
- 490 Turchin, P., 1998. *Quantitative analysis of movement: measuring and modeling population*

REFERENCES

- 491 *redistribution in animals and plants*. Sinauer Associates.
- 492 Wentz, E., Campbell, A., and Houston, R., 2003. A comparison of two methods to cre-
493 ate tracks of moving objects: linear weighted distance and constrained random walk.
494 *International Journal of Geographical Information Science*, 17 (3), 623–645.
- 495 Wilson, R.P., *et al.*, 2007. All at sea with animal tracks; methodological and analytical
496 solutions for the resolution of movement. *Deep Sea Research Part II: Topical Studies*
497 *in Oceanography*, 54 (3-4), 193–210.
- 498 Winter, S. and Yin, Z.C.C., 2010. Directed movements in probabilistic time geography.
499 *International Journal of Geographical Information Science*, 24 (9), 1349–1365.
- 500 Winter, S. and Yin, Z.C.C., 2011. The elements of probabilistic time geography. *Geoin-*
501 *formatica*, 15 (3), 417–434.
- 502 Yu, B. and Kim, S.H., 2006. Interpolating and using most likely trajectories in moving-
503 objects databases. *In: S. Bressan, J. Kung and R. Wagner, eds. DEXA 2006, LNCS*
504 *4080* Springer-Verlag, 718–727.
- 505 Yu, B. and Kim, S., 2004. Curve-based representation of moving object trajectories.
506 *In: International Database Engineering and Applications Symposium (IDEAS) IEEE*
507 Computer Society, p. 7.
- 508 Yuksel, C., Schaefer, S., and Keyser, J., 2011. Parameterization and applications of
509 Catmull-Rom curves. *CAD Computer Aided Design*, 43 (7), 747–755.

Tables and Figures

Table 1: Five interpolation methods employed in this study along with rationale for selection and selected reference(s).

REFERENCES

Method	Rationale	Selected Reference(s)
kinematic	<ul style="list-style-type: none"> – Proposed here. – Uses kinematic motion equations to define interpolation. 	This Paper
linear	<ul style="list-style-type: none"> – Most popular method and most computationally straightforward. – Special case of kinematic interpolation. 	(Wentz <i>et al.</i> 2003, Tremblay <i>et al.</i> 2006)
constrained random walk	<ul style="list-style-type: none"> – Potentially useful for interpolating animal trajectories. – As implemented here, relates to time geographic framework for movement analysis. 	(Wentz <i>et al.</i> 2003, Technitis <i>et al.</i> 2015)
Bézier curve	<ul style="list-style-type: none"> – Demonstrated to be effective in interpolating marine mammals. – Should be appropriate with curvi-linear paths. 	(Tremblay <i>et al.</i> 2006)
Catmull-Rom curve	<ul style="list-style-type: none"> – Special type of cubic interpolating spline commonly used in computer graphics. – Many potential parameterizations, but Catmull-Rom parameterization especially useful in path interpolation. 	(Barry and Goldman 1988)

REFERENCES

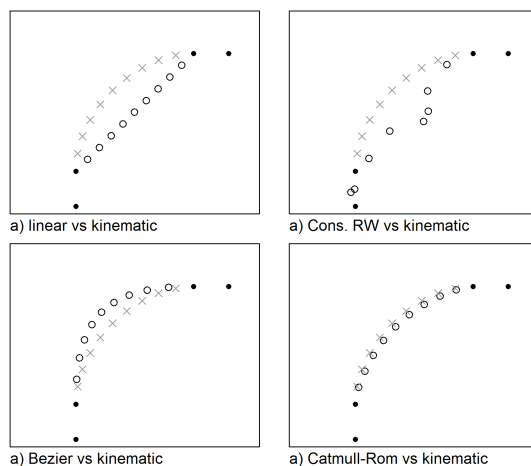


Figure 1. Contrived example of contrasting different path interpolation methods (open circles) with kinematic interpolation (grey crosses), known locations are denoted by filled circles. In the example, the object begins at the point $\mathbf{z}(0) = (0, -3)$ with a velocity of 0 m/s and then moves to the origin $\mathbf{z}(1) = (0, 0)$ with a velocity of 3 m/s to the North $\mathbf{v}(1) = (0, 3)$. The object reaches position $\mathbf{z}(6) = (10, 10)$ after 5 s , it now has a velocity of 3 m/s to the East $\mathbf{v}(6) = (3, 0)$ and it continues on to location $\mathbf{z}(7) = (13, 10)$. The time difference between the initial and final point is 5 s and the object's location is estimated every $1/2 \text{ s}$ in between.

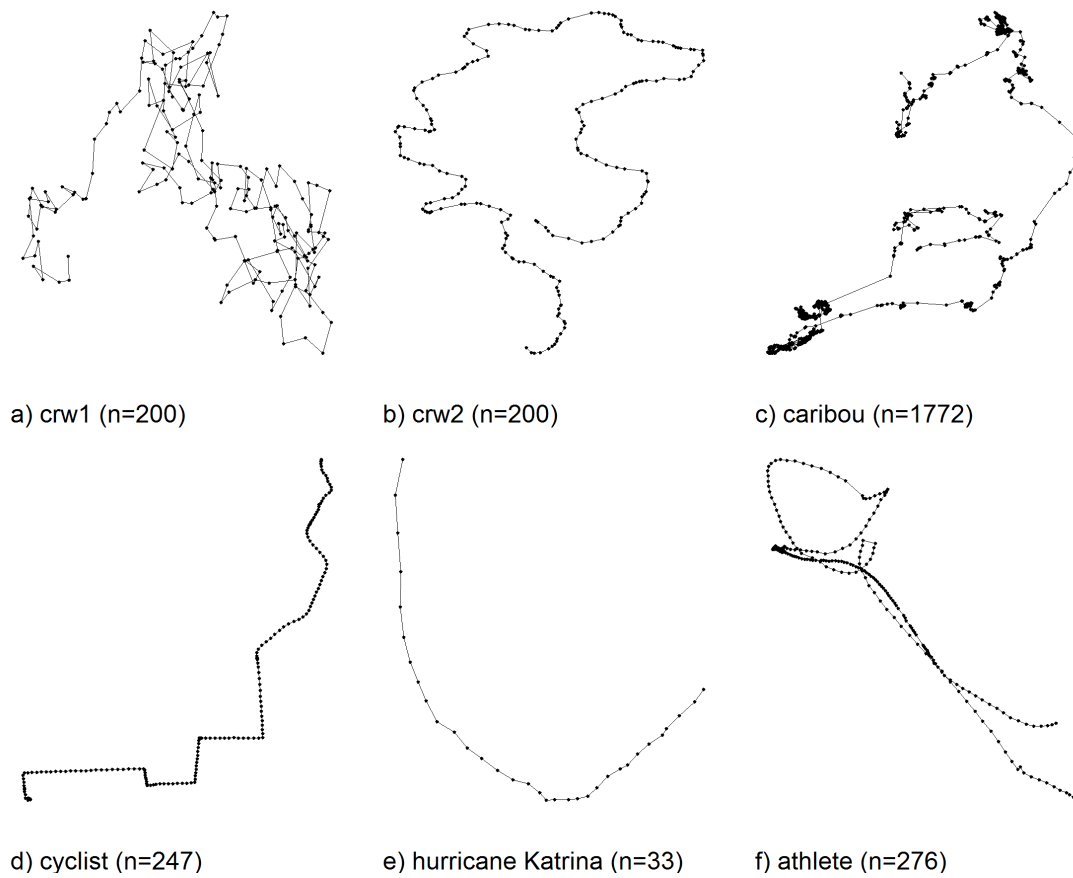


Figure 2. Six empirical datasets used for testing kinematic interpolation: a) crw1 ($n = 200$), b) crw2 ($n = 200$), c) caribou ($n = 1772$), d) cyclist ($n = 246$), e) hurricane Katrina ($n = 33$), f) athlete ($n = 276$).

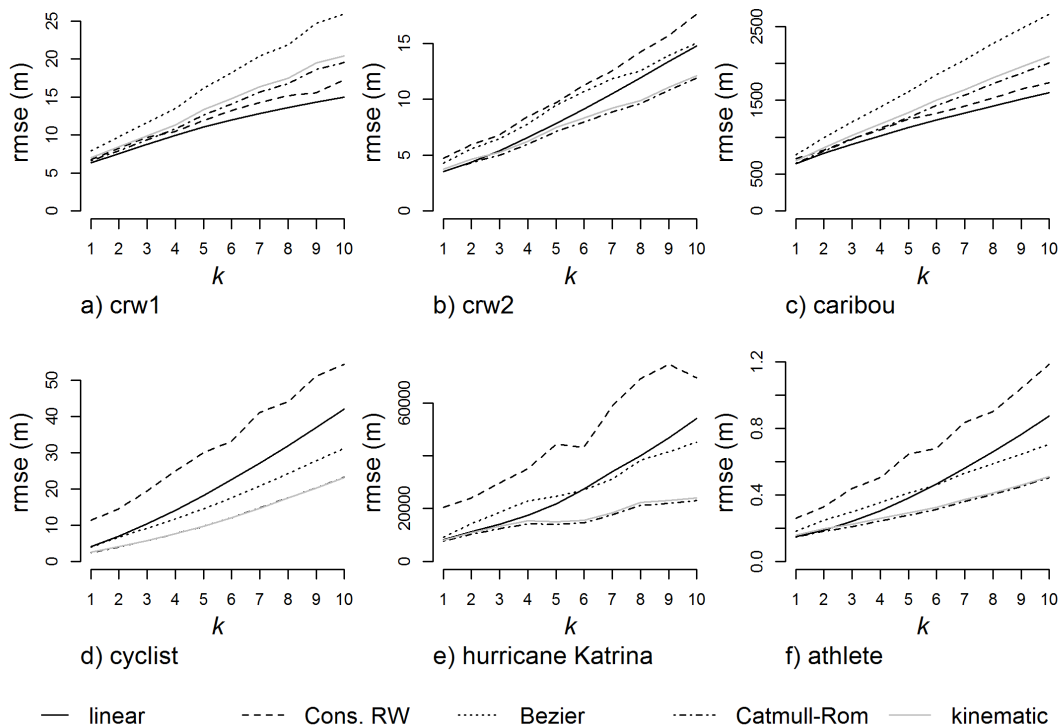


Figure 3. Root mean squared error (rmse; error defined as the euclidean distance between the interpolated and true location) for each interpolation method, for values of k from 1, ..., 10, for each of the six datasets: a) crw1, b) crw2, c) caribou, d) cyclist, e) hurricane Katrina, f) athlete.

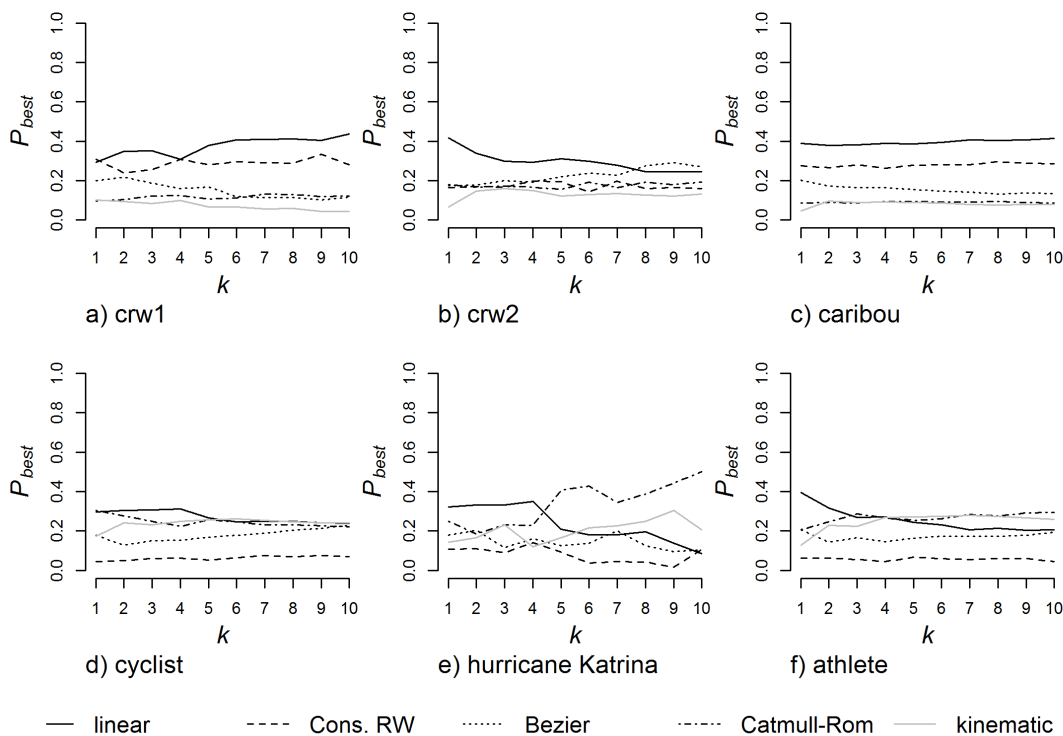


Figure 4. The proportion of interpolations where each method performed best (P_{best}), with values of k from 1, ..., 10, for each of the six datasets: a) crw1, b) crw2, c) caribou, d) cyclist, e) hurricane Katrina, f) athlete.

Supplementary Material A

Derivation of Catmull-Rom curve.

Considering the four points $\mathbf{z}(t_{i-1}), \mathbf{z}(t_i), \mathbf{z}(t_j), \mathbf{z}(t_{j+1})$ where we wish to interpolate the position along the Catmull-Rom curve at t_u where $t_i < t_u < t_j$. The Catmull-Rom interpolation curve for path interpolation takes the following form:

$$\mathbf{z}(t_u) = \frac{t_j - t_u}{t_j - t_i} B1 + \frac{t_u - t_i}{t_j - t_i} B2$$

where

$$B1 = \frac{t_j - t_u}{t_j - t_{i-1}} A1 + \frac{t_u - t_{i-1}}{t_j - t_{i-1}} A2$$

$$B2 = \frac{t_{j+1} - t_u}{t_{j+1} - t_{i-1}} A2 + \frac{t_u - t_i}{t_{j+1} - t_i} A3$$

$$A1 = \frac{t_i - t_u}{t_i - t_{i-1}} \mathbf{z}(t_{i-1}) + \frac{t_u - t_{i-1}}{t_i - t_{i-1}} \mathbf{z}(t_i)$$

$$A2 = \frac{t_j - t_u}{t_j - t_i} \mathbf{z}(t_i) + \frac{t_u - t_i}{t_j - t_i} \mathbf{z}(t_j)$$

$$A3 = \frac{t_{j+1} - t_u}{t_{j+1} - t_j} \mathbf{z}(t_j) + \frac{t_u - t_j}{t_{j+1} - t_j} \mathbf{z}(t_{j+1})$$

Supplementary Material B

Computational efficiency test for each interpolation method, where k represents the number of interpolations performed. From this it can be seen that each of the methods are computed in $O(n)$ time. That is, a ten-fold increase in the number of points to be interpolated, is associated with a ten-fold increase in computation time, in all cases.

k	linear	Bézier	Catmull-Rom	kinematic	constrained RW*
1×10^6	0.017	0.247	0.061	0.124	0.067
1×10^7	0.136	2.261	0.538	1.227	0.676
1×10^8	1.637	23.438	5.283	12.622	6.820
2×10^8	2.981	46.415	10.631	25.137	13.872

*The constrained random walk algorithm is much slower than the other methods, and thus was compared using values of $k = 10, 100, 1000, 2000$.